

Simulation of barotropic wind-driven circulation in the Bay of Bengal and Andaman Sea during premonsoon and postmonsoon seasons

A S Unnikrishnan & N Bahulayan

National Institute of Oceanography, Dona Paula, Goa 403 004, India

Received 11 May 1990; revised 3 September 1990

Two-dimensional vertically integrated model has been used to simulate depth-mean wind-driven circulation during premonsoon and postmonsoon seasons in the upper layers of the Bay of Bengal and Andaman Sea. The model is integrated for 365 d, forced by monthly mean wind stress. The model simulation results show the presence of a large anticyclonic gyre covering the entire Bay of Bengal and a small anticyclonic eddy around Andaman Sea during premonsoon season (March). However, during April, this gyre is seen only in the central and northern parts of the Bay of Bengal. Two anticyclonic gyres are observed in the central and southern parts of the Bay of Bengal during September. During October, the simulated currents are variable in their directions and have low magnitudes.

Circulation in the upper layers of the Bay of Bengal and Andaman Sea (BBAS), is mainly controlled by the prevailing monsoon winds. Previous studies¹ have shown that enormous amount of freshwater discharge from various rivers from the Indian, Bangladesh and Burmese coasts also affect the circulation in the upper layers of the BBAS. There have been some studies pertaining to the modelling of tides and storm surges^{2,3} in the BBAS. Cox⁴ has developed a numerical model of the Indian Ocean including its marginal seas. Bahulayan and Varadachari⁵ have developed a depth-averaged model to simulate wind-driven circulation in the BBAS, forced by winds of constant speed and direction. Later, Bahulayan and Unnikrishnan⁶ have used the same model to simulate the wind-driven circulation in the BBAS, during southwest and northeast monsoon seasons, generated by the observed monthly mean winds.

In this paper, features of simulated wind-driven circulation in the BBAS during premonsoon and postmonsoon seasons using the hydrodynamic model^{5,6} are discussed. Monthly mean wind fields⁷, compiled over 60 y period have been used to drive the model, which is integrated for a period of 365 d to study the seasonal evolution of circulation in the BBAS.

Methods

Computation of depth of wind-driven layer and wind stress—Hydrodynamic model used in the present study may be used in shallow coastal regions and homogeneous water bodies, where vertical variations in density are assumed to be negligible. However, here

only the upper homogeneous layer is considered, which is affected by wind, for the simulation of the depth-mean circulation. The thickness of the upper homogeneous wind-driven Ekman layer, D_E , to a first approximation, is a function of wind speed and latitude of the region and can be expressed⁸ as

$$D_E = 4.3 W / \sqrt{\sin \phi} \quad \dots (1)$$

where W is the wind speed in $\text{m}\cdot\text{sec}^{-1}$ and ϕ is the latitude of the region.

Since the model resolution is $\frac{1}{3}$ rd of a degree in x and y directions, monthly mean wind field was lineally interpolated in space to $\frac{1}{3}$ rd of a degree. The depth of wind-driven layer at each grid point for each month was computed using Eq. 1. If the actual depth at a grid point is less than the computed depth of the wind-driven layer, then the actual depth was taken for the numerical simulation. The monthly mean wind stress components computed from monthly mean wind field are the forcings in the model. The resultant wind stress $|\bar{\tau}|$ was first computed using the relation

$$|\bar{\tau}| = C_D \rho_{\text{air}} |\bar{V}|^2 \quad \dots (2)$$

where ρ_{air} is the density of air and \bar{V} is the monthly mean resultant wind speed. The drag coefficient C_D was computed following the relation⁹

$$C_D = (0.8 + 0.065 |\bar{V}|) 10^{-3} \quad \dots (3)$$

Monthly mean wind stress components τ_x and τ_y were calculated using the relation

$$\tau_x = |\bar{\tau}| \sin \bar{\alpha} \quad \text{and} \quad \tau_y = |\bar{\tau}| \cos \bar{\alpha} \quad \dots (4)$$

where α is the mean wind direction. The wind stress components, taken +ve to the east and north respectively, were computed for each month using Eq. 4.

Premonsoon season (March-April)—During March, southerly and southwesterly winds prevail over the northern part of the BBAS, whereas northerly and northeasterly winds prevail over the southern part of the Bay of Bengal. The magnitude of the winds is of the order of 1-2 m.sec⁻¹. The computed wind stress values (Fig. 1A, B) are generally low in the whole domain and the maximum value observed is 0.009 N.m⁻². During April, the winter monsoon wind pattern gets changed into that characteristic of Asian summer monsoon⁷. Winds with a southerly component approach the western and northern parts of the BBAS, while the eastern part is characterised by northerly and northeasterly winds. The maximum value of the wind stress is of the order of 0.03 N.m⁻², which is noticed in the northern part of the Bay of Bengal (Fig. 1C, D).

Postmonsoon season (September-October)—Monthly mean winds during September are generally southwesterly. Fig. 1E, F show that maximum intensities of wind stress components are found in the southern and central parts of the BBAS (0.05 N.m⁻²). During October, transition from the southwest monsoon to the northeast monsoon takes place and the intensity of winds is very less compared to other months. There is a gradual decrease in the intensity of x and y components of wind stress from the southern side to the northern part of the Bay of Bengal (Fig. 1G and H).

Model equations and numerical procedure—The non-linear vertically integrated equations, used in the present model and their finite difference approximations are given in an earlier work⁵. The model area extends between long. 80°E and 98°E and lat. 6°N and 22°30'N. Andaman and Nicobar islands are represented in the model resolution. This is done between lat. 11°20' and 13°40'N and long 92°20' and 93°E. Since a staggered grid is used, it is necessary to have two grids in the longitude direction to prescribe appropriate boundary conditions. It is justified in view of the very shallow depths observed around the islands. The southern boundary along 6°N is an open boundary. The western, northern and eastern boundaries of the model domain are closed and a zero normal flux condition of $u = v = 0$ is applied depending on the orientation of stair step line segments. Thus, $v = 0$ is applied on those straight line segments that are parallel to x-axis and $u = 0$ is applied on those straight line segments that are parallel to y-axis. For the southern open sea boundary, the sea surface elevation of $\eta = 0$ is applied. In purely wind-driven flow, the clamped boundary condition of $\eta = 0$ can be applied, if the sea

surface is contiguous with deep ocean¹⁰. Few numerical experiments have been made with this model using a radiation type boundary condition and a clamped type, as mentioned above. It is found that the application of the latter is better near the open boundary. Accordingly, boundary condition of $\eta = 0$ has been chosen for the simulation of seasonal circulation. The initial condition is a state of rest i.e., $u = v = \eta = 0$ at $t = 0$.

The hydrodynamic equations are solved numerically subjected to the above mentioned boundary and initial conditions on a 55 × 50 finite difference mesh by means of explicit scheme. The grid resolution is 33.5 and 36.5 km in the x and y directions respectively. The hydrodynamic model, forced with the mean wind stress for January, is integrated from rest at 0000 hrs on 1st January. A time step of 600 sec is chosen for the numerical integration, which satisfied the Courant-Fredrich-Lewy stability criterion given by $\Delta t \leq (\Delta x, \Delta y) (2gh)^{-1/2}$, where Δx and Δy are space steps in x and y directions and h is the maximum depth of wind-driven layer. The model fields spin up very fast and a steady state circulation is attained after approximately 15 d of numerical integration. Keeping the wind stress components for January constant, integration is continued for one month. The simulated model fields at the end of January (31st day) are taken as initial condition for February and the model is integrated till the end of February (28th day), using the mean wind stress components for February as forcing. The sudden change of wind field at the beginning of February has generated initial transients in the solution, which are completely dissipated through friction after about 15 d of integration. By replacing the wind forcing at the beginning of each month with the corresponding monthly mean wind stress components and using the solution obtained at the end of the previous month as initial condition for the subsequent months, integration of model equations is continued till the end of December to study the complete seasonal variability of circulation in the BBAS. In this paper, depth-mean circulation during some selected months only is discussed.

Results and Discussion

There are hardly any observational or modelling studies on circulation covering the entire BBAS over the complete seasonal cycle for comparison with the present model results. The best existing compilation of Indian Ocean surface currents is contained in the Atlas, prepared by Cutler and Swallow¹¹ (hereafter referred to as CS charts) in the form of 10 d averaged values on 1° squares and the charts of surface currents of KNMI¹².

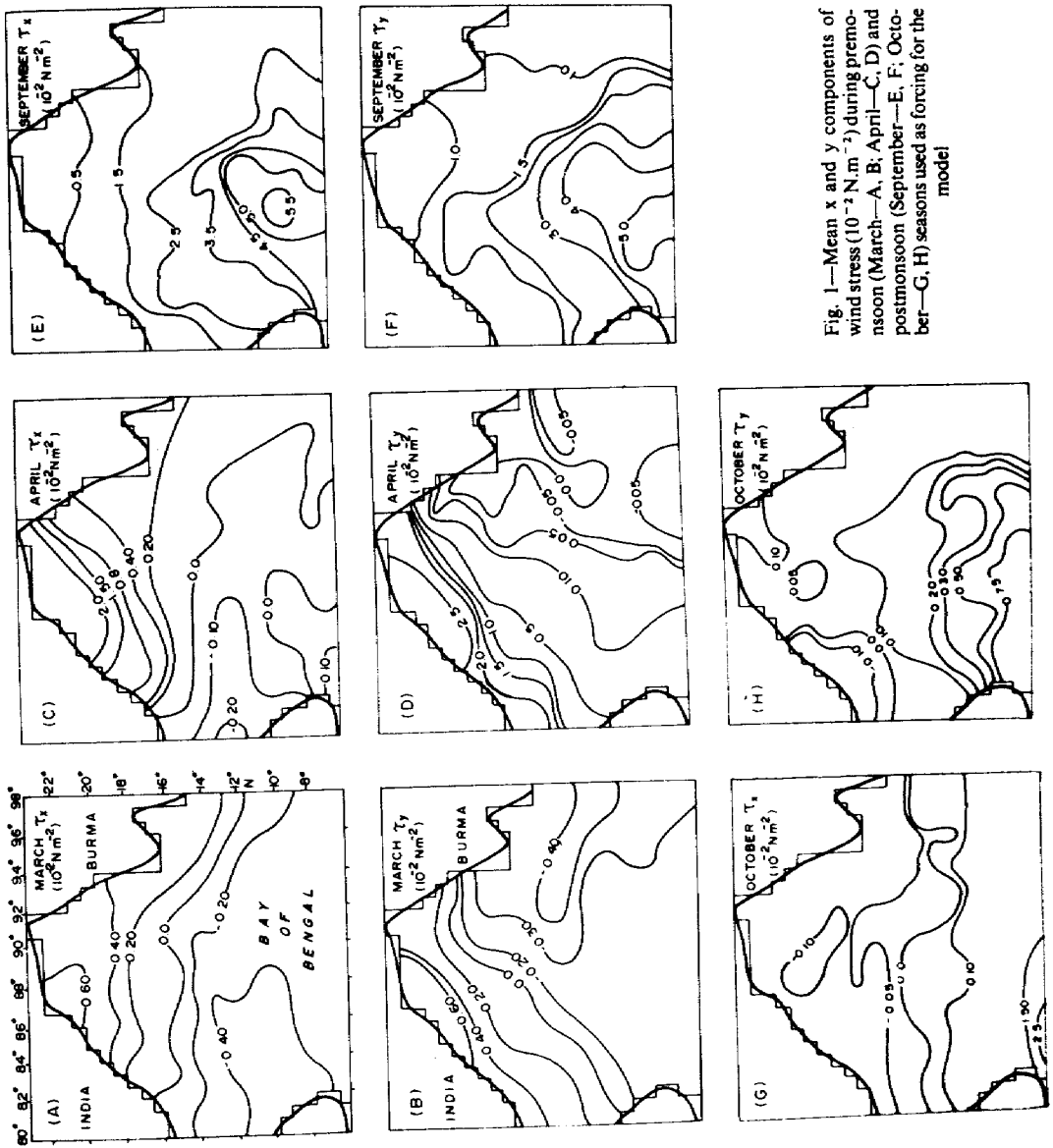


Fig. 1—Mean x and y components of wind stress (10^{-2} N m^{-2}) during pre-monsoon (March—A, B; April—C, D) and post-monsoon (September—E, F; October—G, H) seasons used as forcing for the model

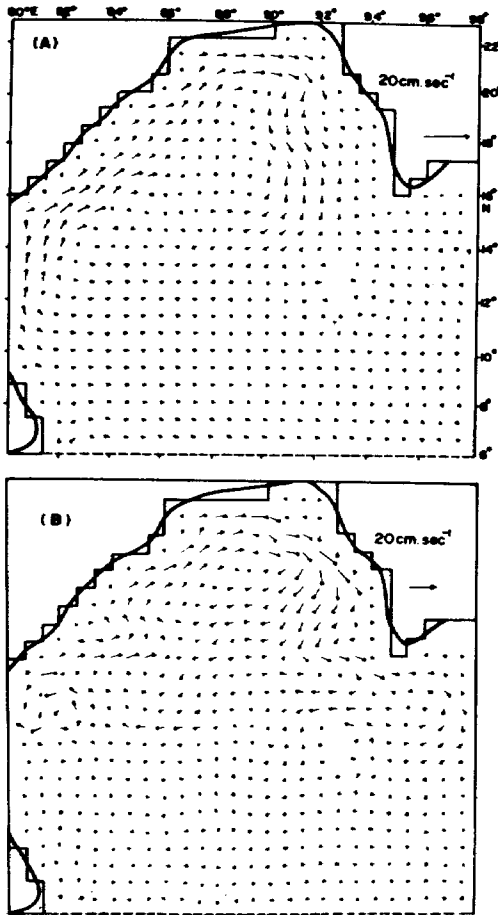


Fig. 2—Simulated depth-mean currents for 31 March (A) and 30 April (B)

Premonsoon circulation—Figs 2A and B show the simulated current field at the end of March and April respectively. During March, a large anticyclonic gyre, covering the entire Bay of Bengal, and a small anticyclonic eddy around the Andaman and Nicobar Islands are observed. In the southern part of the model area, which is the area of the north equatorial current during the premonsoon season, the currents are generally westward. The westward flow in the southern part of the Bay of Bengal turns northwards on reaching the coast of Sri Lanka and then moves in a north, northeasterly direction along the entire east coast of India, as a strong western boundary current. This current flows towards east on reaching the head of the Bay of Bengal, moves southwards along the Burmese coast and then joins with the westerly flow in the southeastern part of the Bay of Bengal. Thus a large anticyclonic gyre is formed covering the entire Bay of Bengal.

By 30 April (Fig. 2B), the western boundary current along the east coast of India, which is a part of the large anticyclonic gyre formed in the Bay of Bengal, is considerably weakened due to reduction of wind speeds in the central and the southern parts of the model area. The size of this large anticyclonic gyre is also considerably decreased and it is shifted towards north. In general, the intensity of currents in the southern part of the Bay of Bengal is reduced towards the end of April.

The charts of surface currents¹² for the second half of March and April also show a clockwise circulation in the entire Bay of Bengal. The KNMI charts of currents for the second half of March and April also show a large anticyclonic circulation in the entire Bay of Bengal. A strong northward flowing western boundary current, which is a part of the above mentioned anticyclonic gyre, is observed along the east coast of India during March. The magnitude of this western boundary current exceeds 50 cm. sec^{-1} in the northern part of the Bay of Bengal. The model simulation results for the 30th March (Fig. 2A) also show the existence of a large anticyclonic gyre covering the entire Bay of Bengal. The strong northward flowing western boundary current along the east coast of India is reproduced in the present model simulation. However, by 30 April (Fig. 2B), the anticyclonic gyre gets shifted towards the northern part of the Bay of Bengal.

Postmonsoon circulation—Figs 3A and B show simulated circulation towards the end of September and October respectively. During September, the monthly mean winds over the area continue to be southwesterly. Two anticyclonic gyres found in the central and southern parts of the Bay of Bengal during southwest monsoon⁶ are still present. However, the intensities of currents are lower than those during southwest monsoon. The simulated currents during the transition month of October are variable in direction and their magnitudes are very low. Along the east coast of India, the currents are directed southward during October.

The CS charts for the 3rd part of September show, in general, an eastward drift in the central part of the Bay of Bengal. The monsoon drift current is still prevalent in the equatorial region between 3° - 7° N and along the east coast of India, currents are southward. In general, the magnitudes of currents are of 10 cm. sec^{-1} or less except near the Sri Lanka, where they are of the order of 50 cm. sec^{-1} . The charts of surface currents¹² for September show a cyclonic circulation in the northern part of the Bay of Bengal. During October, 2 cyclonic gyres are observed in the northern and southwestern parts of the Bay of Bengal.

In the simulated circulation for the 30 September (Fig. 3A), the above mentioned observed features of

circulation such as the eastward drift in the central part of the Bay of Bengal, cyclonic type of circulation in the northern part, etc. can be noticed. However, in the simulated results, the southward flow along the east coast of India is clearly seen in October only. In October, the simulated currents are very weak. In fact, monthly mean wind speeds are very low during this period.

Acknowledgement

All the computations have been carried out in the ND-520 computer and the help rendered by the staff of the Computer Division is acknowledged. Thanks are due to the Director and Head, Physical Oceanography Division for encouragement.

References

- 1 Panakala Rao D & Sastry J S, *Mahasagar—Bull Natn Inst Oceanogr*, 4 (1981) 1.
- 2 Johns B, Dube S K, Mohanty U C & Sinha P C, *Quart J R Meteorol Soc*, 107 (1981) 919.
- 3 Murty T S, *Storm surges—Meteorological Ocean Tides*, Canad Bull Fish Aquatic Sciences 212 (Department of Fisheries and Oceans, Ottawa), 1984, pp. 897.
- 4 Cox M D, *Deep-Sea Res*, 17 (1970) 47.
- 5 Bahulayan N & Varadachari V V R, *Indian J Mar Sci*, 15 (1986) 8.
- 6 Bahulayan N & Unnikrishnan A S (Communicated).
- 7 Hastenrath S & Lamb P J, *Climatic atlas of the Indian Ocean. Part I: Surface climate and atmospheric circulation* (University of Wisconsin Press, Wisconsin), 1979, pp. 97.
- 8 Pond S & Pickard G L, *Introductory dynamical oceanography* (Pergamon Press, Oxford), 1983, pp. 329.
- 9 Wu J, *J Phy Oceanogr*, 10 (1980) 727.
- 10 Fandry C B, *Aust J Mar Fresh Wat Res*, 32 (1981) 9.
- 11 Cutler A N & Swallow J C, *Surface currents of the Indian Ocean*, Report No. 187 (Institute of Oceanographic Sciences, Wormley), 1984, pp. 81.
- 12 Anonymous, *Indian Ocean oceanographic and meteorologic data*, Publication No. 135 (Koninklijk Netherlands Meteorological Institute, Verkruglaarlig), 1952.

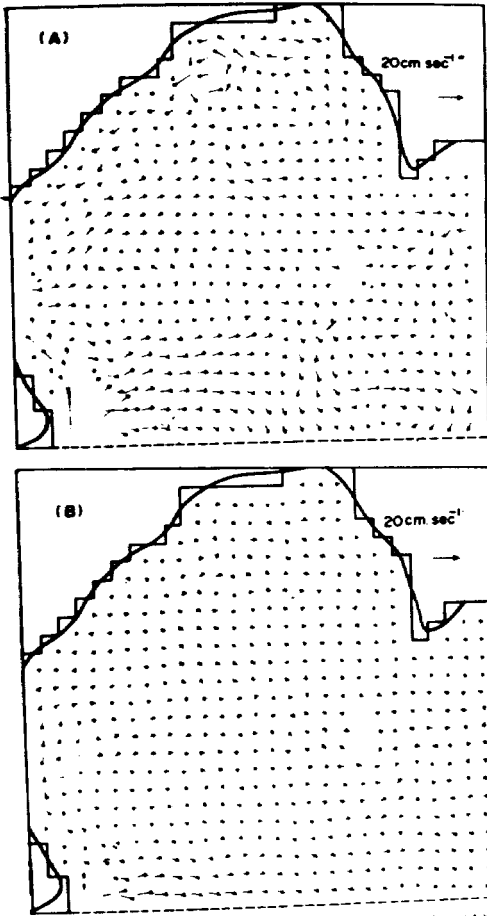


Fig. 3—Simulated depth-mean currents for 30 September (A) and 31 October (B)